*Work supported by the U. S. Atomic Energy Commission.

[1]F. W. Bingham, Phys. Rev. 182, 180 (1969).
[2]F. W. Bingham, Phys. Rev. A 2, 1365 (1970).
[3]E. J. Knystautas, Q. C. Kessel, R. Del Boca, and H. C. Hayden, Phys. Rev. A 1, 825 (1970).
[4]F. W. Bingham, J. Chem. Phys. 46, 2003 (1967).
[5]N. Bohr, Phys. Rev. 59, 270 (1941).
[6]F. Herman and S. Skillman, *Atomic Structure Calculations* (Prentice-Hall, Englewood Cliffs, N. J., 1963).
[7]W. Lichten, Phys. Rev. 164, 131 (1967).
[8]J. K. Rice and F. W. Bingham (unpublished).
[9]J. A. Bearden and A. F. Burr, Rev. Mod. Phys. 39, 125 (1967).

PHYSICAL REVIEW A VOLUME 4, NUMBER 3 SEPTEMBER 1971

Relativistic Treatment of the Excitation of Characteristic L X Rays by the Impact of Heavy Charged Particles*

Byung-Ho Choi
Physics Department, University of North Carolina, Chapel Hill, North Carolina 27514
(Received 1 March 1971)

The cross sections for L electron ionization by incident heavy, but slow, charged particles are evaluated. Incident particles are described in the plane-wave Born approximation, while relativistic wave functions are used for the atomic electrons. Numerical results are given for holmium and mercury and compared with experimental data for holmium. The results are discussed.

I. INTRODUCTION

The inner-shell ionization of atoms due to collisions with incident heavy charged particles has been studied by several authors in the past. [1]

The emission of characteristic x rays following the creation of a vacancy in an inner shell has received attention from both atomic and nuclear physicists.

The differential energy-transfer cross sections for this process provide the basis for calculations of stopping power when a heavy charged particle penetrates through matter and are useful in the study of radiation damage to solids or biological specimens. They also have been investigated by some authors to test the more detailed comparison between experiment and theory. [2-4]

Calculations of the differential and total ionization cross sections and of the inner-shell contributions to the stopping power have usually been made in the nonrelativistic plane-wave Born approximation. [5-7]

In this approximation, apart from the use of plane waves for the incident projectile, nonrelativistic hydrogenic wave functions are employed for the atomic electrons.

However, for the heavier elements the relativistic bound-state wave functions are considerably different from those of the nonrelativistic theory. Not only are the former larger in magnitude than the latter near the nucleus but also the energy differences between atomic subshells are significant and affect the calculations of the ionization cross section. Hence, relativistic considerations are desirable for treating both K and L electrons of the medium-heavy and heavy elements.

Moreover, the energy spectrum of fast electrons emitted from the inner atomic shells should be described relativistically for any element. For the K-shell ionization, such a calculation was made by Jamnik and Zupančič[8] employing Dirac wave functions for the bound and ejected atomic electrons. They found good agreement between theoretical and experimental K-shell ionization cross sections for heavy elements such as Ag and Pb. Experimental data exist on L-shell ionization cross sections for certain elements[9] and there is thus an incentive for performing calculations which take into account the relativistic description of the atomic L electrons. In this paper, we have evaluated the relativistic L-shell ionization cross section following the scheme of calculations of Jamnik and Zupančič.

In Sec. II, the method is outlined that provides expressions for the form factors for the transition from each L subshell to both discrete and continuum final states.

Sample results of the present calculations were tabulated and presented in graphical form for comparison with experimental data. The results are discussed in Sec. III.

II. RELATIVISTIC IONIZATION CROSS SECTION

The energy-transfer cross section for the ejection of atomic electrons by incident heavy charged particles is given by

$$\frac{d\sigma_{if}}{dE_f} = \frac{4\pi}{\hbar^2} z^2 e^2 \frac{M}{E} \int_{q_{\min}}^{q_{\max}} \frac{dq}{q^3} \left| F_{if}(q) \right|^2 \qquad (1)$$

in the nonrelativistic plane-wave Born approxima-

tion, where $\vec{q}$ is the momentum transferred to the atomic electrons, ze and M are the charge and the mass of the incident particle, and E and E_f are the energies of the incident particle and ejected electrons, respectively.

The square of the form factor $|F_{if}(q)|^2$ for the transition between the initial and the final electronic states, $\psi_i(\vec{r})$ and $\psi_f(\vec{r})$, is defined to be

$$|F_{if}(q)|^2 = \left| \int e^{i\vec{q}\cdot\vec{r}} \psi_f(\vec{r})^* \psi_i(\vec{r})\, d^3\vec{r} \right|^2 .$$

For the wave functions of atomic electrons which were initially bounded and finally ejected from the L shell, we have used the Coulomb solutions of the Dirac equation in the form

$$\psi = \begin{cases} -if_\kappa(r)\, \mathcal{Y}^{j_z}_{l(-\kappa)1/2,j}(\theta,\varphi) \\ g_\kappa(r)\, \mathcal{Y}^{j_z}_{l(\kappa)1/2,j}(\theta,\varphi), \quad \kappa = \mp 1, \mp 2, \ldots \end{cases}$$

where $\mathcal{Y}^{j_z}_{l1/2,j}(\theta,\varphi)$ are the Pauli's two-component spin-wave functions.

The angular momentum j of the electrons is given by

$$j = |\kappa| - \tfrac{1}{2} \quad \text{and} \quad l(\kappa) = \begin{cases} \kappa & \text{for } \kappa > 0 \\ |\kappa| - 1 & \text{for } \kappa < 0. \end{cases}$$

The relativistic radial wave functions $f_\kappa(r)$ and $g_\kappa(r)$ for the discrete and continuum states, normalized per unit energy interval, are given in the literature.[8,10–12] (For continuum states, the wave functions normalized per energy interval in units of $Z_L^2 R_\infty$ have been used in the present calculation. Z_L is the effective nucelar charge number seen by the L electrons.)

The angular integrations were carried out through the use of the algebra of vector coupling and Raccah coefficients. Summing over the initial and the final magnetic quantum numbers, we obtain for the L subshell

$$\begin{aligned} |F_{L_1,W_{L_1}}(q)|^2 &= 2 \sum_{\kappa_f = \mp 1, \mp 2, \ldots} |\kappa_f| [J^{(l_1)}_{L_1,\kappa_f}(q)]^2, \\ |F_{L_2,W_{L_2}}(q)|^2 &= 2 \sum_{\kappa_f = \mp 1, \mp 2, \ldots} |\kappa_f| [J^{(l_2)}_{L_2,\kappa_f}(q)]^2, \\ |F_{L_3,W_{L_3}}(q)|^2 &= 2 \sum_{\kappa_f = \mp 1, \mp 2, \ldots} \{A(\kappa_f)[J^{(l_3)}_{L_3,\kappa_f}(q) \\ &\quad + J^{(l_4)}_{L_3,\kappa_f}(q)]^2 + B(\kappa_f)[\lambda(\kappa_f) J^{(l_3)}_{L_3,\kappa_f}(q) \\ &\quad + \mu(\kappa_f) J^{(l_4)}_{L_3,\kappa_f}(q)]^2\}, \end{aligned} \tag{2}$$

where $W_{L_{1,2,3}}$ signifies the energies transferred to the atomic electrons of each L subshell by the incident particle in units of $Z_L^2 R_\infty$,

$$J^{(l_i)}_{L_s,\kappa_f}(q) = \int j_{l_i}(qr)[f_{\kappa_f}(r) f_{L_s}(r) + g_{\kappa_f}(r) g_{L_s}(r)]\, r^2 dr, \tag{3}$$

with $l_1 = l(\kappa_f)$, $l_2 = l(-\kappa_f)$, $l_3 = l(\kappa_f) - 1$, $l_4 = l(\kappa_f) + 1$,

$$A(\kappa) = \begin{cases} \frac{3}{2} \dfrac{\kappa(\kappa^2-1)}{(2\kappa+1)^2} & \text{for } \kappa > 0 \\ \frac{3}{2} \dfrac{|\kappa|(|\kappa|^2-1)}{(2|\kappa|-1)^2} & \text{for } \kappa < 0, \end{cases}$$

$$B(\kappa) = \begin{cases} \dfrac{\kappa}{2(2\kappa+1)^2} & \text{for } \kappa > 0 \\ \dfrac{|\kappa|}{2(2|\kappa|-1)^2} & \text{for } \kappa < 0, \end{cases}$$

$$\lambda(\kappa) = \begin{cases} \kappa - 1 & \text{for } \kappa > 0 \\ 3(|\kappa| - 1) & \text{for } \kappa < 0, \end{cases}$$

and

$$\mu(\kappa) = \begin{cases} -3(\kappa+1) & \text{for } \kappa > 0 \\ -(|\kappa|+1) & \text{for } \kappa < 0. \end{cases}$$

For the radial integration J, we again follow the method of Jamnik and Zupančič.[8] The final results for L electrons are as follows (we express the momentum transfer q in units of Z_L/a_0 hereafter):

$$\begin{aligned} J^{(l_1)}_{L_1,\kappa_f}(q) &= \sqrt{\pi}\, \frac{\Gamma(2a_1)}{2^{l_1+1}}\, D_{L_1} D_f \\ &\quad \times \exp[-(\gamma_1 + \gamma_{\kappa_f} + 1)\ln q] F_1(q), \\ J^{(l_2)}_{L_2,\kappa_f}(q) &= \sqrt{\pi}\, \frac{\Gamma(2a_2)}{2^{l_2+1}}\, D_{L_2} D_f \\ &\quad \times \exp[-(\gamma_1 + \gamma_{\kappa_f} + 1)\ln q] F_2(q), \\ J^{(l_3)}_{L_3,\kappa_f}(q) &= \sqrt{\pi}\, \frac{\Gamma(2a_3)}{2^{l_3+1}}\, D_{L_3} D_f \\ &\quad \times \exp[-(\gamma_2 + \gamma_{\kappa_f} + 1)\ln q] F_3(q), \\ J^{(l_4)}_{L_3,\kappa_f}(q) &= \sqrt{\pi}\, \frac{\Gamma(2a_4)}{2^{l_4+1}}\, D_{L_3} D_f \\ &\quad \times \exp[-(\gamma_2 + \gamma_{\kappa_f} + 1)\ln q] F_4(q), \end{aligned} \tag{4}$$

where

$$\gamma_\kappa = [\kappa^2 - (\alpha Z_L)^2]^{1/2},$$

$$\alpha = e^2/\hbar c \qquad \text{(fine-structure constant)},$$

$$a_i = \tfrac{1}{2}(\gamma_1 + \gamma_{\kappa_f} + l_i + 1) \quad \text{for } i = 1, 2,$$

$$a_i = \tfrac{1}{2}(\gamma_2 + \gamma_{\kappa_f} + l_i + 1) \quad \text{for } i = 3, 4,$$

$$D_f = \frac{1}{2\sqrt{\pi}} \frac{\exp[(\gamma_{\kappa_f} - \frac{1}{2})\ln 2k]}{\Gamma(2\gamma_{\kappa_f}+1)} e^{\pi w/2k} \left|\Gamma\left(\gamma_{\kappa_f} + \frac{iw}{k}\right)\right|,$$

$$w = E_f/mc^2 = [1 + (\alpha Z_L)^2 k^2]^{1/2}$$

for the continuum final states, and

$$D_f = D(n', \kappa_f)$$

$$= \frac{\exp[(\gamma_{\kappa_f} - \frac{1}{2})\ln 2]}{\exp[(\gamma_{\kappa_f}+1)\ln N_f]\,\Gamma(2\gamma_{\kappa_f}+1)} \times \left(\frac{\Gamma(2\gamma_{\kappa_f}+n'+1)}{\Gamma(n'+1)(N_f - \kappa_f)}\right)^{1/2},$$

$$N_f = (n'^2 + \kappa_f^2 + 2n'\gamma_{\kappa_f})^{1/2}$$

for the discrete final states;

$$D_{L_1} = D(1, -1), \quad D_{L_2} = D(1, 1), \quad D_{L_3} = 4D(0, -2),$$

$$F_1(q) = A_1 \sum_m (-1)^m P_m^{(1)} q^{-2m} + B_1 \sum_m (-1)^m Q_m^{(1)} \times q^{-(2m+1)} + C_1 \sum_m (-1)^m R_m^{(1)} q^{-(2m+1)} + D_1 \sum_m (-1)^m S_m^{(1)} q^{-(2m+2)},$$

$$F_2(q) = A_2 \sum_m (-1)^m P_m^{(2)} q^{-2m} + B_2 \sum_m (-1)^m Q_m^{(2)} \times q^{-(2m+1)} + C_2 \sum_m (-1)^m R_m^{(2)} q^{-(2m+1)} + D_2 \sum_m (-1)^m S_m^{(2)} q^{-(2m+2)},$$

$$F_3(q) = A_3 \sum_m (-1)^m P_m^{(3)} q^{-2m} + B_3 \sum_m (-1)^m Q_m^{(3)} q^{-(2m+1)},$$

$$F_4(q) = A_4 \sum_m (-1)^m P_m^{(4)} q^{-2m} + B_4 \sum_m (-1)^m Q_m^{(4)} q^{-(2m+1)},$$

where

$$A_i = \frac{\Gamma(\frac{1}{2})}{\Gamma(a_i + \frac{1}{2})\,\Gamma(1 - b_i)}, \quad B_i = \frac{\Gamma(-\frac{1}{2})}{\Gamma(a_i)\,\Gamma(\frac{1}{2} - b_i)} \quad \text{for } i = 1, 2, 3, 4,$$

with

$$b_i = \tfrac{1}{2}(\gamma_1 + \gamma_{\kappa_f} - l_i) \quad \text{for } i = 1, 2,$$

$$b_i = \tfrac{1}{2}(\gamma_2 + \gamma_{\kappa_f} - l_i) \quad \text{for } i = 3, 4,$$

$$C_1 = \frac{2(1+1/N)}{2\gamma_1+1} B_1, \quad D_1 = -\frac{8a_1b_1(1+1/N)}{2\gamma_1+1} A_1,$$

$$C_2 = \frac{2(1-1/N)}{2\gamma_1+1} B_2, \quad D_2 = -\frac{8a_2b_2(1-1/N)}{2\gamma_1+1} A_2,$$

with

$$N = [2(1+\gamma_1)]^{1/2},$$

$$P_m^{(i)} = \frac{(a_i)_m (b_i)_m}{(\frac{1}{2})_m m!} p_m^{(i)}, \qquad Q_m^{(i)} = \frac{(a_i + \frac{1}{2})_m (b_i + \frac{1}{2})_m}{(\frac{3}{2})_m m!} q_m^{(i)} \quad \text{for } i = 1, 2, 3, 4,$$

$$R_m^{(i)} = \frac{(a_i + \frac{1}{2})_m (b_i + \frac{1}{2})_m}{(\frac{1}{2})_m m!} r_m^{(i)}, \quad S_m^{(i)} = \frac{(a_i + 1)_m (b_i + 1)_m}{(\frac{3}{2})_m m!} s_m^{(i)} \quad \text{for } i = 1, 2$$

For the continuum final states,

$$p_m^{(i)} = 2\,\mathrm{Re}[U_{2m}(\kappa_f, k, N) G_i] \quad \text{for } i = 1, 2,$$
$$q_m^{(i)} = 2\,\mathrm{Re}[U_{2m+1}(\kappa_f, k, N) G_i] \quad \text{for } i = 1, 2,$$
$$r_m^{(i)} = 2\,\mathrm{Re}[U_{2m}(\kappa_f, k, N) H_i] \quad \text{for } i = 1, 2,$$
$$s_m^{(i)} = 2\,\mathrm{Re}[U_{2m+1}(\kappa_f, k, N) H_i] \quad \text{for } i = 1, 2,$$
$$p_m^{(i)} = 2\,\mathrm{Re}[U_{2m}(\kappa_f, k, 2) G_i] \quad \text{for } i = 3, 4,$$
$$q_m^{(i)} = 2\,\mathrm{Re}[U_{2m+1}(\kappa_f, k, 2) G_i] \quad \text{for } i = 3, 4,$$

where

$$U_n(\kappa_f, k, N) = {}_2F_1\left(-n, \gamma_{\kappa_f} + 1 + \frac{iw}{k}, 2\gamma_{\kappa_f} + 1, \frac{2ik}{1/N + ik}\right)\left(\frac{1}{N} + ik\right)^n,$$

$$G_1 = e^{i\eta}(\gamma_{\kappa_f} + iw/k)\,[N(1+\theta_{L_1})^{1/2}(w+1)^{1/2} - i(N+2)(1-\theta_{L_1})^{1/2}(w-1)^{1/2}],$$

$$G_2 = e^{i\eta}(\gamma_{\kappa_f} + iw/k)\,[(N-2)(1+\theta_{L_2})^{1/2}(w+1)^{1/2} - iN(1-\theta_{L_2})^{1/2}(w-1)^{1/2}],$$

$$G_3 = G_4 = e^{i\eta}(\gamma_{\kappa_f} + iw/k)\,[(1+\theta_{L_3})^{1/2}(w+1)^{1/2} - i(1-\theta_{L_3})^{1/2}(w-1)^{1/2}],$$

$$H_1 = H_2 = e^{i\eta}(\gamma_{\kappa_f} + iw/k)\,[(1+\theta_{L_1})^{1/2}(w+1)^{1/2} - i(1-\theta_{L_1})^{1/2}(w-1)^{1/2}],$$

$$e^{2i\eta} = -\frac{\kappa_f - i/k}{\gamma_{\kappa_f} + iw/k}, \quad (a)_m = \frac{\Gamma(a+m)}{\Gamma(a)}.$$

For the discrete final states,

$$p_m^{(i)} = I_i V_{2m}(\kappa_f, n', N, N_f) + J_i V_{2m}(\kappa_f, n'+1, N, N_f) \quad \text{for } i = 1, 2$$

$$q_m^{(i)} = I_i V_{2m+1}(\kappa_f, n', N, N_f) + J_i V_{2m+1}(\kappa_f, n'+1, N, N_f) \quad \text{for } i = 1, 2,$$

$$r_m^{(i)} = K_i V_{2m}(\kappa_f, n', N, N_f) + M_i V_{2m}(\kappa_f, n'+1, N, N_f) \quad \text{for } i = 1, 2,$$

$$s_m^{(i)} = K_i V_{2m+1}(\kappa_f, n', N, N_f) + M_i V_{2m+1}(\kappa_f, n'+1, N, N_f) \quad \text{for } i = 1, 2,$$

$$p_m^{(i)} = I_i V_{2m}(\kappa_f, n', 2, N_f) + J_i V_{2m}(\kappa_f, n'+1, 2, N_f) \quad \text{for } i = 3, 4,$$

$$q_m^{(i)} = I_i V_{2m+1}(\kappa_f, n', 2, N_f) + J_i V_{2m+1}(\kappa_f, n'+1, 2, N_f) \quad \text{for } i = 3, 4,$$

where

$$V_n(\kappa_f, n', N, N_f) = {}_2F_1\left(-n, -n'+1, 2\gamma_{\kappa_f}+1, \frac{2/N_f}{1/N+1/N_f}\right)\left(\frac{1}{N}+\frac{1}{N_f}\right)^n,$$

$$I_1 = n'[(N+2)(1-\theta_{L_1})^{1/2}(1-\theta_f)^{1/2} - N(1+\theta_{L_1})^{1/2}(1+\theta_f)^{1/2}],$$

$$I_2 = n'[N(1-\theta_{L_2})^{1/2}(1-\theta_f)^{1/2} - (N-2)(1+\theta_{L_2})^{1/2}(1+\theta_f)^{1/2}],$$

$$I_3 = I_4 = n'[(1-\theta_{L_3})^{1/2}(1-\theta_f)^{1/2} - (1+\theta_{L_3})^{1/2}(1+\theta_f)^{1/2}],$$

$$J_1 = (N_f - \kappa_f)[(N+2)(1-\theta_{L_1})^{1/2}(1-\theta_f)^{1/2} + N(1+\theta_{L_1})^{1/2}(1+\theta_f)^{1/2}],$$

$$J_2 = (N_f - \kappa_f)[N(1-\theta_{L_2})^{1/2}(1-\theta_f)^{1/2} + (N-2)(1+\theta_{L_2})^{1/2}(1+\theta_f)^{1/2}],$$

$$J_3 = J_4 = (N_f - \kappa_f)[(1-\theta_{L_3})^{1/2}(1-\theta_f)^{1/2} + (1+\theta_{L_3})^{1/2}(1+\theta_f)^{1/2}],$$

$$K_1 = K_2 = n'[(1-\theta_{L_1})^{1/2}(1-\theta_f)^{1/2} - (1+\theta_{L_1})^{1/2}(1+\theta_f)^{1/2}],$$

$$M_1 = M_2 = (N_f - \kappa_f)[(1-\theta_{L_1})^{1/2}(1-\theta_f)^{1/2} + (1+\theta_{L_1})^{1/2}(1+\theta_f)^{1/2}],$$

$$\theta_f = \theta(n', \kappa_f) = [1 + (\alpha Z_L)^2/(n'+\gamma_{\kappa_f})^2]^{-1/2},$$

$$\theta_{L_1} = \theta(1, -1), \quad \theta_{L_2} = \theta(1, 1) = \theta_{L_1}, \quad \theta_{L_3} = \theta(0, -2).$$

The energy transfers W_{L_i} are given as

$$W_{L_i} = 2(w - \theta_{L_i})/(\alpha Z_L)^2,$$

$$W_{L_i} = 2(\theta_f - \theta_{L_i})/(\alpha Z_L)^2$$

for the continuum and discrete final states, respectively. The relativistic energy distribution of each L-subshell electron is given by

$$\frac{d\sigma_{L_i}}{dW_{L_i}} = \frac{8\pi z^2 a_0^2}{Z_L^4 \eta_L} I_{L_i}(\eta_L, W_{L_i}), \tag{5}$$

with

$$I_{L_i}(\eta_L, W_{L_i}) = \frac{1}{2}\int_{q_{\min}}^{q_{\max}} \frac{dq}{q^3} |F_{L_i, W_{L_i}}(q)|^2,$$

$$\eta_L = \frac{E}{(M/m)Z_L^2 R_\infty}.$$

$I_{L_i}(\eta_L, W_{L_i})$ is called the excitation function of the L_i subshell.[1] The total ionization cross section of L electrons is obtained by integrating the energy distributions over W_{L_i}, i.e.,

$$\sigma_L = \sigma_{L_1} + \sigma_{L_2} + \sigma_{L_3},$$

$$\sigma_{L_i} = \int_{W_{L_i,\min}}^{\infty} \frac{d\sigma_{L_i}}{dW_{L_i}} dW_{L_i}, \tag{6}$$

where $W_{L_i,\min}$ is the observed ionization potential of the L_i subshell.[13] This, then, takes into account the screening effects due to the outer electrons and $|F_{L_i, W_{L_i}}(q)|^2$ for $W_{L_i} < 2(1-\theta_{L_i})/(\alpha Z_L)^2$ is given by Eqs. (2)–(4) for the discrete final states, with n' considered to be a continuous variable, multiplied by the factor

TABLE I. Sample numerical results of the relativistic excitation functions for Hg($Z=80$), $\eta_L=0.004$, $\eta_L=0.007$ as functions of the energy transfers W_{L_i}. See the text for the definition of W_{L_i}.

W_{L_1}	I_{L_1}	W_{L_2}	I_{L_2}	W_{L_3}	I_{L_3}
			$\eta_L=0.004$		
0.18	3.9751×10^{-3}	0.18	5.8063×10^{-3}	0.16	2.4994×10^{-2}
0.20	3.0902×10^{-3}	0.20	2.5615×10^{-3}	0.18	1.0459×10^{-2}
0.22	2.2262×10^{-3}	0.22	1.1905×10^{-3}	0.20	4.6078×10^{-3}
0.24	1.5383×10^{-3}	0.24	5.7638×10^{-4}	0.22	2.1084×10^{-3}
0.26	1.0420×10^{-3}	0.26	2.9048×10^{-4}	0.24	1.0046×10^{-3}
0.27	8.5482×10^{-4}	0.27	2.0911×10^{-4}	0.25	7.0347×10^{-4}
[a]					
0.285	6.3224×10^{-4}	0.285	1.2929×10^{-4}	0.26	4.9556×10^{-4}
0.315	3.4659×10^{-4}	0.315	5.2054×10^{-5}	0.29	1.8217×10^{-4}
0.405	6.5805×10^{-5}	0.405	5.0085×10^{-6}	0.35	3.0727×10^{-5}
			$\eta_L=0.007$		
0.18	6.8690×10^{-3}	0.18	4.7077×10^{-2}	0.16	1.7319×10^{-1}
0.20	4.6548×10^{-3}	0.20	2.3080×10^{-2}	0.18	8.2832×10^{-2}
0.22	4.2510×10^{-3}	0.22	1.1840×10^{-2}	0.20	4.1787×10^{-2}
0.24	3.8244×10^{-3}	0.24	6.2012×10^{-3}	0.22	2.1298×10^{-2}
0.26	3.2300×10^{-3}	0.26	3.3406×10^{-3}	0.24	1.1134×10^{-2}
0.27	2.9087×10^{-3}	0.27	2.4767×10^{-3}	0.25	8.1249×10^{-3}
[a]					
0.285	2.4290×10^{-3}	0.285	1.5932×10^{-3}	0.26	5.9449×10^{-3}
0.315	1.6119×10^{-3}	0.315	6.8553×10^{-4}	0.29	2.4096×10^{-3}
0.405	4.2617×10^{-4}	0.405	7.4681×10^{-5}	0.35	4.6652×10^{-4}

[a] These spaces divide the discrete and continuum final states.

$$\frac{dn'}{dW_{L_i}}=\left(1+\frac{(\alpha Z_L)^2}{(n'+\gamma_{\kappa_f})^2}\right)^{3/2}\ \tfrac{1}{2}(n'+\gamma_{\kappa_f})^3\ .$$

For evaluating the energy distribution, we have squared the series in the form-factor expressions and integrated over q term by term algebraically. Thus the numerical work leads to summation of the series in negative powers of $q_{\min}$, which considerably reduces the laborious work. In general, the numerical accuracy of the present calculation is better than 1%.

TABLE II. Relativistic cross sections, in units of a_0^2, as a function of the proton incident energy $\eta_L=E/[(M/m)Z_L{}^2R_\infty]$.

Element	η_L	σ_L/a_0^2
Ho	0.001	8.29×10^{-9}
	0.003	2.40×10^{-7}
	0.004	5.29×10^{-7}
	0.005	9.47×10^{-7}
	0.006	1.49×10^{-6}
	0.007	2.14×10^{-6}
Hg	0.001	3.51×10^{-9}
	0.002	2.79×10^{-8}
	0.003	8.87×10^{-8}
	0.004	1.94×10^{-7}
	0.005	3.47×10^{-7}
	0.006	5.47×10^{-7}
	0.007	7.95×10^{-7}

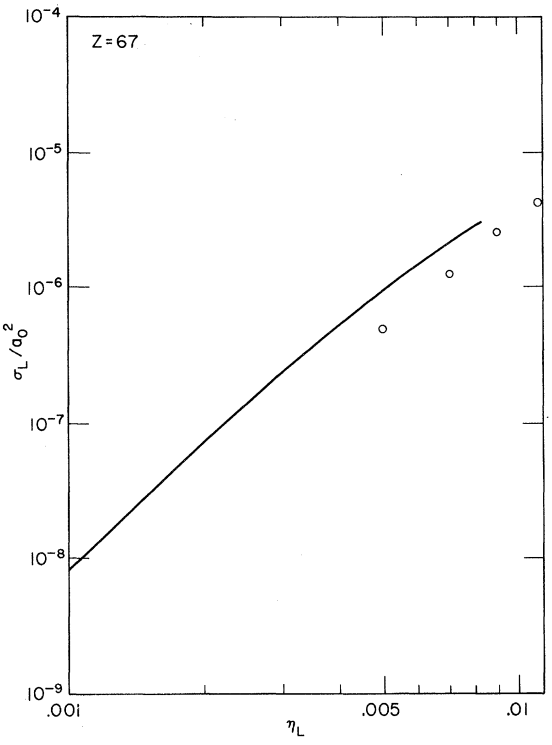

FIG. 1. Relativistic L-shell ionization cross section σ_L in units of a_0^2 (solid line) for holmium compared with experimental data (marked by O) as a function of incident proton energy in units of $(M/m)Z_L^2R_\infty$. Experimental data were taken from Ref. 9.

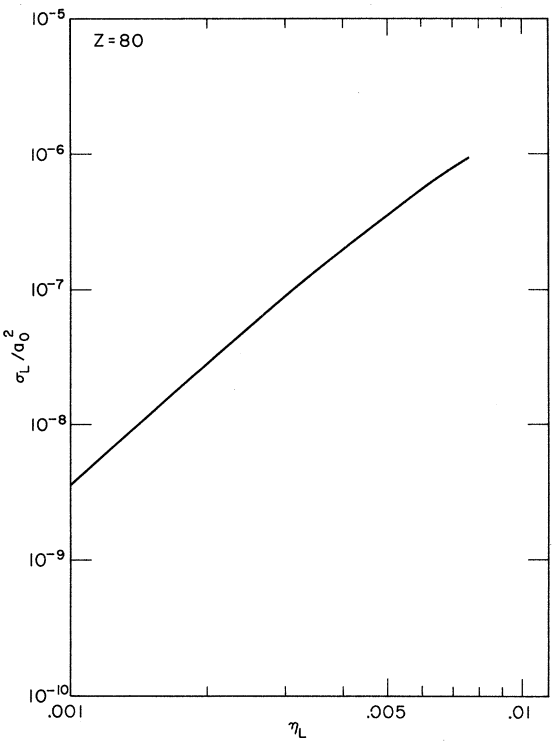

FIG. 2. Relativistic L-shell ionization cross section σ_L in units of a_0^2 for mercury as a function of incident proton energy in units of $(M/m)Z_L^2R_\infty$.

III. RESULTS AND DISCUSSIONS

The relativistic cross section for the L-shell ionization by collisions of incident heavy charged particles was computed for several values of incident energies up to $\eta_L = 0.007$ and for several species of target atoms.

It was found that at most eight partial waves ($\kappa_f = \mp 8$) were needed for reasonable accuracy in the calculation.

A separate program similarly yielded numerical results for the relativistic excitation functions, etc., for K-shell ionization, employing the form factors given by Jamnik and Zupančič and reproducing their tabulated values.[8]

For purposes of illustration, a few sample numerical results for the excitation functions of each L subshell are presented in Table I for mercury using an effective $Z_L = 75.85$. It should be noted that the relativistic excitation functions as functions of η_L, W_{L_i} also separately depend on Z_L, while the nonrelativistic excitation functions do not explicitly depend on Z_L. We have compared our results for the excitation functions with the nonrelativistic plane-wave Born approximation calculations. In the low-energy-transfer region, the two excitation functions are not significantly different and for a certain incident energy, the relativistic excitation functions are even slightly smaller than those of the nonrelativistic calculation near $W_{L_i} \simeq W_{L_i,\min}$.

On the other hand, in the large energy-transfer region, the relativistic excitation functions are always larger than the nonrelativistic ones and this discrepancy becomes significant for heavy elements.

This can be understood from the fact that, for large energy transfers, the momentum transfer q becomes large. Hence, the contributions to the integration in Eq. (3) mainly arise from the region quite close to the nucleus. Since the bound-state relativistic wave functions are much larger than those of the nonrelativistic theory near the nucleus, the relativistic excitation functions are significantly increased for large energy transfers.

It can be seen also from Table I that much more than half of the contribution to the total cross section comes from the discrete final states. It is interesting to note that the transition between the discrete and continuum final states is very smooth.

The relativistic cross sections for the L-shell ionization of holmium ($Z = 67$) and mercury ($Z = 80$) are presented in Table II.

In Fig. 1, calculations are compared with experimental data for holmium given by Khan *et al.*[9] Calculations for mercury are shown in Fig. 2 for comparison with experimental data.

Here $\eta_L = 0.007$ corresponds to approximately 700 keV and 1 MeV of the proton incident energy for holmium and mercury, respectively. For holmium, the agreement between theoretical results and experimental data in the high incident energies are somewhat better than in the low-incident-energy region.

Yet, the discrepancy between experiment and theory is still considerable.

This might arise partly from the use of the plane wave for the incident particle, that is, the neglect of deflection effects due to Coulomb repulsion between the incident particle and the atomic nucleus.

Computations for the K- and L-shell contributions to the stopping numbers[14] have also been made using the relativistic excitation functions. However, in the energy range below 1 MeV and for high Z, the K- and L-shell contributions to the stopping numbers are negligible. Relativistic cross section for the L-shell ionization by an impact of heavy charged particles, obtaining the explicit expression for the form factors, Eqs. (2)–(4), are the results of this paper.

The relativistic effect on the electronic wave functions for the L-shell ionization process are significant for heavy elements, comparing the relativistic excitation functions with the nonrelativistic ones. Therefore, it will be interesting to compare the relativistic theory with the experimental data on the L-shell ionization cross sections for heavy elements

(say, $Z \geq 80$) in the present incident-energy range.[15]

ACKNOWLEDGMENTS

The author should like to express his sincere gratitude to Professor Eugen Merzbacher for his helpful discussions and suggestions. The author is also grateful to Dr. Govind S. Khandelwal for his suggestions.

*Work supported in part by the U. S. Atomic Energy Commission under Contract No. AT-(40-1)-2408.

[1]For a summary of both the experimental and the theoretical aspects of x-ray production by heavy charged particles, cf. E. Merzbacher and H. W. Lewis, in *Handbuch der Physik*, edited by S. Flügge (Springer-Verlag, Berlin, 1958), Vol. 34, p. 166.

[2]T. Huus, J. H. Bjerregaard, and B. Elbek, Kgl. Danske Videnskab. Selskab, Mat.-Fys. Medd. 30, No. 17 (1956).

[3]C. Zupančič and T. Huus, Phys. Rev. 94, 205 (1954).

[4]B. H. Choi and E. Merzbacher, Phys. Rev. 177, 233 (1969).

[5]H. A. Bethe, Ann. Phys. (Leipzig) 5, 325 (1930).

[6]M. C. Walske, Phys. Rev. 101, 940 (1956).

[7]G. S. Khandelwal and E. Merzbacher, Phys. Rev. 144, 349 (1966).

[8]D. Jamnik and C. Zupančič, Kgl. Danske Videnskab. Selskab, Mat.-Fys. Medd. 31, No. 2 (1957).

[9]J. M. Khan, D. L. Potter, and R. D. Worley, Phys. Rev. 139, A1735 (1965).

[10]H. A. Bethe, in *Handbuch der Physik*, edited by H. Geiger and Karl Scheel (Springer-Verlag, Berlin, 1933), Vol. XXIV/1.

[11]M. E. Rose, Phys. Rev. 51, 484 (1937).

[12]M. E. Rose and R. K. Osborn, Phys. Rev. 93, 1315 (1954).

[13]For recent compilations of the observed ionization potential, see J. A. Bearden and A. F. Burr, Rev. Mod. Phys. 39, 125 (1967).

[14]For nonrelativistic calculations of stopping numbers, see J. O. Hirschfelder and J. L. Magee, Phys. Rev. 73, 207 (1948) and Refs. 5–7.

[15]Our computer programs for the relativistic ionization cross sections and stopping numbers were made for arbitrary elements. The author can provide numerical results for any elements upon request.

PHYSICAL REVIEW A VOLUME 4, NUMBER 3 SEPTEMBER 1971

Low-Energy Electron Scattering in the Random-Phase Approximation

Barry Schneider and Joel I. Krugler
GTE Laboratories, Incorporated, Bayside, New York 11360
(Received 29 March 1971)

A general formalism for the computation of low-energy inelastic and elastic electron scattering cross sections within the context of the particle-hole Bethe-Salpeter equation is presented and shown to reduce to the random-phase approximation (RPA) in lowest order. The theory is then applied to triplet elastic electron-He^+ scattering. A short discussion of the differences between the RPA for scattering processes and for low-lying bound states is given, and the numerical methods used to solve the equations are considered in some detail in an appendix.

I. INTRODUCTION

One of the major problems associated with low-energy elastic and inelastic electron scattering from atomic systems is the role of electron correlations. Straightforward application of the close-coupling formalism of Burke and Schey,[1–3] while quite successful in predicting scattering cross sections, requires a great deal of computational effort. Although a number of new numerical techniques adapted to handling large numbers of coupled differential equations,[4,5] or in some way circumventing their direct solution,[6] have reduced the time needed to obtain cross sections, there are still considerable difficulties when there are large numbers of exchange terms. One of the basic difficulties associated with low-energy electron scattering is the need to antisymmetrize the total scattering wave function. In configuration space this necessitates the inclusion of large numbers of nonlocal potentials in each scattering channel. An alternative to this procedure is to introduce creation and destruction operators as in field theory and utilize the formalism of modern many-body theory.[7,8] Such methods have been used quite successfully in nucleon scattering by systems of identical nucleons and, as we shall show, exhibit promise in electron scattering problems. In this article we present a discussion of inelastic and elastic scattering which in lowest approximation reduces to the solution of the eigenvalue problem of the random-phase approximation (RPA).[9–11] The for-